# Taxon-specific hydrogen isotope signals in cultures and mesocosms facilitate ecosystem and hydroclimate reconstruction

S. Nemiah Ladd[a, b]*, Daniel B. Nelson[b, c], Blake Matthews[d], Shannon Dyer[b], Romana Limberger[e,f], Antonia Klatt[a], Anita Narwani[g], Nathalie Dubois[h, i], Carsten J. Schubert[b, j],

[a] University of Basel, Department of Environmental Sciences, Basel, Switzerland
[b] Swiss Federal Institute of Aquatic Science and Technology (EAWAG), Department of Surface Waters – Research and Management, Kastanienbaum, Switzerland
[c] University of Basel, Department of Environmental Sciences – Botany, Basel, Switzerland
[d] Swiss Federal Institute of Aquatic Science and Technology (EAWAG), Department of Fish Ecology and Evolution, Kastanienbaum, Switzerland
[e] Swiss Federal Institute of Aquatic Science and Technology (EAWAG), Department of Aquatic Ecology, Kastanienbaum, Switzerland
[f] University of Zürich, Department of Evolutionary Biology and Environmental Studies, Zürich, Switzerland
[g] Swiss Federal Institute of Aquatic Science and Technology (EAWAG), Department of Aquatic Ecology, Dübendorf, Switzerland
[h] Swiss Federal Institute of Aquatic Science and Technology (EAWAG), Department of Surface Waters – Research and Management, Dübendorf, Switzerland
[i] Swiss Federal Institute of Technology (ETH-Zürich), Department of Earth Sciences, Zürich, Switzerland
[j] Swiss Federal Institute of Technology (ETH-Zürich), Department of Environmental Systems Science, Zürich, Switzerland

*Corresponding author: n.ladd@unibas.ch, +41 61 207 36 27

Co-author email addresses: daniel.nelson@unibas.ch, Blake.Matthews@eawag.ch, shannon.dyer15@gmail.com, romana.limberger@ieu.uzh.ch, antonia.klatt@unibas.ch, Anita.Narwani@eawag.ch, Nathalie.Dubois@eawag.ch, Carsten.Schubert@eawag.ch

**This manuscript has been submitted for peer review at *Geochimica et Cosmochimica Acta*. Subsequent versions following peer review may differ slightly in content. The authors welcome feedback on this version.**

**Abstract**

Phytoplankton play a key role in biogeochemical cycles, impacting atmospheric and aquatic chemistry, food webs, and water quality. However, it remains challenging to reconstruct changes in algal community composition throughout the geologic past, as existing proxies are suitable only for a subset of taxa and/or influenced by degradation. Here, we investigate if compound-specific hydrogen isotope ratios ($\delta^2H$ values) of common algal lipids can serve as (paleo)ecological indicators. First, we grew 20 species of algae – representing cyanobacteria, diatoms, dinoflagellates, green algae, and cryptomonads – in batch cultures under identical conditions and measured $\delta^2H$ values of their lipids. Despite identical source water $\delta^2H$ values, lipid $\delta^2H$ values ranged from -455 ‰ to -52 ‰, and clustered according to taxonomic groups and chemical compound classes. In particular, green algae synthesized fatty acids with higher $\delta^2H$ values than other taxa, cyanobacteria synthesized phytol with relatively low $\delta^2H$ values, and diatoms synthesized sterols with higher $\delta^2H$ values than other eukaryotes. Second, we assessed how changes in algal community composition can affect net $\delta^2H$ values of common algal lipids in 20 experimental outdoor ponds, which were manipulated via nutrient loading, and the addition of macrophytes and mussels. High algal biomass in the ponds, which was mainly caused by cyanobacterial and green algal blooms, was associated with higher $\delta^2H$ values for generic fatty acids, relatively stable $\delta^2H$ values for phytol and the dinoflagellate biomarker dinostanol, and lower $\delta^2H$ values for the more cosmopolitan sterol stigmasterol. These results are consistent with expectations from our culture-based analyses, suggesting that measuring $\delta^2H$ values of multiple lipids from sediment and calculating $^2H$-offsets between them can resolve changes in algal community composition from changes in source water isotopes. With an appropriate availability of sedimentary lipids, this approach could permit the reconstruction of both taxonomic variability and hydroclimate from diverse sedimentary systems.

**Key words:** algae, ecohydrology, hydrogen isotopes, lipid biomarkers

## 1. Introduction

Anthropogenic perturbations of carbon, nitrogen, and phosphorus cycling have had profound impacts on aquatic ecosystems, and both eutrophication and global warming have changed the composition and relative abundance of phytoplankton taxa in marine and freshwater systems over the past decades (Diaz and Rosenberg, 2008; Monchamp et al., 2018; Markelov et al., 2019). These changes in phytoplankton community composition

subsequently impact nutrient cycling, food webs, and water quality within aquatic systems, including freshwater lakes (Rabalais et al., 2010; Hixson and Arts, 2016; Huisman et al., 2018). Contextualizing these changes in relation to natural climate and biogeochemical forcings, as well as in response to pre-industrial human impacts is important to better understand and predict the consequences of current human activities on aquatic systems (Haas et al., 2019; Nwosi et al., 2023).

Various sedimentological proxies are available to reconstruct past changes in algal ecology, each with its own strengths and limitations. Classical paleolimnological approaches involve counting fossilized remains of individual taxa, including diatom frustules, dinoflagellate cysts, and cyanobacterial akinetes (Livingstone and Jaworski, 1980; Stoermer et al., 1985; Dixit et al., 1992; Lotter, 1998; Gosling et al., 2020). While these microscopic analyses can provide a high degree of taxonomic precision, they are limited to organisms that produce suitable remains, and many ecologically important taxa including picocyanobacteria and most green algae are missing from such reconstructions. Recent advances in the analysis of sedimentary ancient DNA (sedaDNA) also provide the opportunity for highly-resolved ecological reconstructions (Stoof-Leichsenring et al., 2015; Monchamp et al., 2018; Nwosi et al., 2023), but questions remain about biases introduced from selective preservation of DNA in the sediment and/or amplification of specific DNA fragments during sample processing (Pawlowski et al., 2017; Strivens et al., 2018; Vasselon et al., 2018; Thorpe et al., 2024), as well as the long-term applicability of sedaDNA on geologic time scales (Boere et al., 2011; Kirkpatrick et al., 2016). The relative distribution of pigments and lipid biomarkers in sediments are informative about changes in the abundance of broader algal taxonomic groups (Leavitt and Findlay, 1994; Schubert et al., 1998; Volkman, 2003; Naeher et al., 2012; McGowan et al., 2012; Bauersachs et al., 2017), but these analyses can also be affected by selective degradation (Leavitt and Hodgson, 2002; Bianchi et al., 2002; Reuss et al., 2005).

Another possible approach for reconstructing past changes in algal community structure is based on hydrogen isotopes of common algal lipids, such as phytol, the side-chain moiety of chlorophyll, and $C_{16:0}$ fatty acid (palmitic acid). Hydrogen isotopes of these compounds and other, more source-specific lipid biomarkers ($\delta^2H_{lipid}$ values) have primarily been investigated as proxies for the hydrogen isotopic composition of source water ($\delta^2H_{water}$ values) (Huang et al., 2004; Sachse et al., 2004; Sachse et al., 2012; Maloney et al., 2019; Weiss et al., 2019). Additionally, culturing and field studies have demonstrated that $^2H/^1H$ fractionation between lipids and source water ($\alpha^2H_{Lipid/Water}$ values) are sensitive to a variety

of factors including salinity (Schouten et al., 2006; Sachse and Sachs, 2008; Nelson and Sachs, 2014), light availability (van der Meer et al., 2015; Sachs et al., 2017), and growth rate (Schouten et al., 2006; Z. Zhang et al., 2009; Sachs and Kawka, 2015). However, in a limited number of laboratory studies where multiple species of algae have been cultured under identical conditions, large differences in $\alpha^2H_{Lipid/Water}$ values have been observed among different species (Sessions et al., 1999; Schouten et al., 2006; Zhang and Sachs, 2007; Z. Zhang et al., 2009; Heinzelmann et al., 2015). Each of these investigations included only a small number of species, and was not designed to specifically determine how $\delta^2H_{lipid}$ values differ among algal taxonomic groups, but the differences among taxa were large relative to plausible changes in $\delta^2H_{water}$ values in natural settings.

Empirical calibrations of the relationship between $\delta^2H_{lipid}$ values and $\delta^2H_{water}$ values in natural systems have frequently observed large variability in hydrogen isotope fractionation between lipids and water (e.g., Nelson and Sachs., 2014; Ladd et al., 2017; Ladd et al., 2018; Ladd et al., 2021a). This variability differs in magnitude and, in some cases, in sign among lipids of different compound classes, which could be due to differences in the types of algae contributing lipids to sediments (Ladd et al., 2018; Ladd et al., 2021a). This suggestion has not yet been systematically evaluated, but if $\delta^2H_{lipid}$ values consistently vary among algae taxonomic groups, it would facilitate reconstructions of past changes in algal community composition, as these ubiquitous compounds are found in diverse sedimentary archives (Meyers, 1997; Casteñada and Schouten, 2011; Witkowski et al., 2018). In particular, comparing changes in relative offsets among $\delta^2H_{lipid}$ values from different compound classes could allow changes in community composition to be assessed independently from changes in $\delta^2H_{water}$ values. Another key advantage of this approach in the context of paleoecology is that isotopic composition of hydrogen bound to carbon is stable at the temperatures and pressures found near Earth's surface and sedimentary deposits prior to catagenesis (Schimmelmann et al., 2006).

To investigate how hydrogen isotope fractionation for diverse lipids varies among different types of algae, we grew 20 different species of algae, representing five taxonomic groups, under identical conditions and measured the $\delta^2H$ values of each lipid they produced in high quantities. We then evaluated how differences in algal community structure, observed in 20 outdoor experimental ponds (15000 L), can be translated into net $\delta^2H_{lipid}$ values of common and source-specific specific lipids recovered from suspended particles. We use the results of these laboratory and outdoor experiments to present a conceptual framework for

how algal $\delta^2H_{lipid}$ values can be combined with $\delta^2H$ values from other biomarkers co-occurring in sediment samples to disentangle ecological and hydroclimatic signals.

## 2. Methods

### *2.1 Phytoplankton cultures*

We grew 20 species of phytoplankton (**Table S1**) in batch cultures at Eawag in Kastanienbaum, Switzerland, in 1 L Erlenmeyer flasks at 15 °C under a 12-hour light/dark cycle. Light intensity ranged from 130 - 230 µmol $m^{-2}$ $s^{-1}$ depending on the proximity to the light bank, but culture locations were rotated daily to promote more uniform light distribution among cultures. All cultures were grown on WC medium (Guillard and Lorenzen, 1972), which we prepared from stock nutrient solutions. After the medium for each flask was prepared, we adjusted the pH to 7 and then autoclaved prior to inoculation. We inoculated new cultures from established cultures growing under identical conditions. We monitored cell density on alternating days by removing small volume test aliquots from each culture under sterile conditions and then analyzing by flow cytometry (BD Accuri C6, BD Biosciences, San Jose, CA, USA). We determined cell density at the transition to stationary phase with initial cultures of each species, and then harvested individual cultures during the late exponential growth stage when they were approaching this cell density. Cultures were harvested by filtering them onto 142 mm diameter, 0.7 µm pore-size Whatman® GF/F glass fiber filters (previously combusted at 450 °C), which were stored at -20 °C until analyses were performed. We collected water samples for later analysis of the medium water $\delta^2H$ and $\delta^{18}O$ values on alternating days under the same conditions used to collect cell density aliquots.

### *2.2 Experimental Ponds*

We collected experimental pond samples as part of a large-scale eutrophication experiment that was designed to test the impact of nutrient loading perturbations on interactions between algae, macrophytes, and mussels. This experiment was conducted at the Eawag Experimental Ponds facility in Dübendorf, Switzerland in 2016 (47.405 °N, 8.609 °E), and has previously been described in more detail (Narwani et al., 2019; Lürig et al., 2021). Each of the 20 artificial ponds used in the experiment had a volume of 15,000 L, a maximum depth of 1.5 m, and was inoculated with an algal community derived from surface waters of a nearby lake, Greifensee (47.354 °N, 8.672 °E). We randomly assigned the 20

ponds into five treatments (i.e., four ponds per treatment). Four ponds received neither nutrients, macrophytes, nor mussels (i.e., oligotrophic controls). The remaining 16 ponds received the same nutrient loading treatment over the course of the experiment (Narwani et al., 2019; Lürig et al., 2021), and, at the initiation of the experiment, four ponds received Macrophytes (*Myriophillum spicatum*), four ponds received mussels (*Dreissena polymorpha*), four ponds received both macrophytes and mussels, and four ponds received neither macrophytes and mussels (control ponds with nutrients).

We equipped the 16 ponds that received nutrient additions with Exo2 Sondes (YSI, Yellow Springs, OH, USA) that measured dissolved oxygen, conductivity, temperature, pH, fluorescence of dissolved organic matter, and chlorophyll fluorescence at 15-minute intervals. To these ponds, nitrate and phosphate were added in the form of $KNO_3$ and $K_2HPO_4$ at double the Redfield Ratio (N:P = 32:1), and as pulses of increasing P concentration over time: 10 µg/L (August 12$^{th}$), then 20 µg/L (August 26$^{th}$), 30 µg/L (September 9$^{th}$), and finally 40 µg/L (September 22$^{nd}$, 2016).

On August 23$^{rd}$, September 13$^{th}$, and October 5$^{th}$, 2016, we collected 15 L of water from each pond, using a PVC tube (5 cm diameter, 180 m length) equipped with a stopper and pull-cord, which allowed the entire water column to be sampled. To prevent cross-contamination during sampling, each pond had its own PVC tube sampler and water collection bucket. Water was filtered through identical filters to those used for batch cultures until either the entire 15 L had been filtered, or until the filter clogged. Filters were stored frozen at -20 °C prior to freeze-drying. We also collected 8 mL of filtered water for isotopic analysis from each pond on each sampling date. Water samples were stored in the dark at room temperature in glass screw-cap vials that were sealed with electrical tape.

Throughout the summer and fall, depth-integrated pond water was collected using the same PVC tubes every week, along with samples for nutrient analyses, chlorophyll concentrations, algal cell counts, and flow cytometry (Narwani et al., 2019). Methodology for these analyses and resulting data were published by Narwani et al. (2019).

*2.3 Lipid processing*

We extracted and purified lipids from all samples following previously described protocols (Ladd et al., 2017; Ladd et al., 2021b). In brief, freeze-dried filters were microwave extracted (SOLVpro, Anton Paar, Graz, Austria) in 9:1 dichloromethane (DCM)/methanol (MeOH) at 70 °C and the resulting TLE was saponified in 1N KOH in MeOH (3 hours at 70 °C). We separated neutral lipids and fatty acids from each other by extracting the saponified

sample with hexane, then acidifying it to pH < 2 and extracting again with hexane. We methylated fatty acids with 5 % HCl in MeOH (12 hours at 70 °C). We separated neutral lipids from pond samples into compound classes using silica gel column chromatography, and acetylated 95 % of the resulting alcohol fraction with acetic anhydride in pyridine (30 minutes at 70 °C). We acetylated 95 % of the neutral fraction from batch culture samples under identical conditions.

We quantified lipids by gas chromatography – flame ionization detection (GC-FID) (Shimazdu, Kyoto, Japan) at Eawag in Kastanienbaum, Switzerland, as described by Ladd et al. (2017). We used internal recovery standards that we added prior to lipid extraction to account for any losses during sample handling. We identified fatty acids based on retention times relative to compounds in a fatty acid standard mixture (Supelco 37 component FAME mix, SigmaAldrich). We identified phytosterols and stanols from pond samples by gas chromatography – mass spectrometry (GC-MS) (Agilent Technologies, Santa Clara, CA, USA) at Eawag in Dübendorf, Switzerland, as described by Krentscher et al. (2019). In order to confirm compound identifications, we silylated the 5 % reserve aliquots of the alcohol fraction from each pond sample (25 µL BSTFA in 25 µL pyridine at 60 °C for 1 hour). We compared mass spectra from the resulting trimethylsilyl-ethers to published spectra, and used diagnostic fragments and relative peak areas to confirm identifications of acetylated alcohols, many of which did not have published reference spectra. We identified acetylated sterols from algal cultures by GC-MS (Shimazdu, Kyoto, Japan) at Eawag in Kastanienbaum as described by Ladd et al (2017), comparing resulting mass spectra to those previously identified from pond samples.

### *2.4 Lipid $\delta^2H$ measurements*

We measured compound specific hydrogen isotopes by gas chromatography–isotope ratio mass spectrometry (GC-IRMS) at Eawag in Kastanienbaum on a Trace 1310 GC coupled to a Delta V Plus IRMS with a ConFlow IV interface (Thermo Scientific, Waltham MA, USA), following methods previously described by Ladd et al., (2018). We analyzed a mix of *n*-alkanes of known $\delta^2H$ values (*n*-$C_{17, 19, 21, 23, 25, 28, 34}$) from Arndt Schimmelmann (Indiana University) as reference materials in triplicate at the beginning and end of each sequence, as well as after every 8-9 injections of samples. All sample and standard compound $\delta^2H$ values were initially calculated in the Isodat software platform relative to $H_2$ reference gas. After measurement, the $\delta^2H$ values of the standards were used to reference the sample

compound $\delta^2H$ values to the VSMOW scale and to correct for isotope effects associated with retention time, peak area, or time-based drift. We analyzed an additional quality control standard of *n*-$C_{29}$ alkane three times throughout each sequence ($\delta^2H$ = –139 ± 4.8 ‰; n = 98). The $H_3^+$ factor was calculated at the beginning of each sequence and averaged 3.9 ± 0.4 during the analyses of culture samples and 2.6 ± 0.1 during the analyses of pond samples.

We limited our analysis to compounds with peak areas greater than 15 Vs. Our analyses were generally limited to compounds that produced baseline separated peaks at this concentration on the GC-IRMS, with the exception being unsaturated $C_{18}$ FAMEs, which were manually integrated as a three-compound co-eluting peak, and subsequently referred to as $C_{18:x}$. In the pond samples, the presence and relative abundance of sterols, stanols, and FAMEs was highly variable among samples, and components that were suitable for compound-specific isotopic analyses according to our criteria were not consistent among samples.

*2.5 Water isotope measurements*

We filtered water samples through a 0.45 μm polyethersulfone membrane and analyzed their isotopic composition ($\delta^2H$, $\delta^{18}O$) by cavity ring down spectroscopy (L-2120i Water Isotope Analyzer, Picarro, Santa Clara, CA) at ETH-Zürich as in Ladd et al. (2018). Chem correct software was actively used to flag samples with potential organic contamination. Average offsets from known values for standards analyzed with samples were 0.6 ‰ for hydrogen and 0.1 ‰ for oxygen. Average standard deviations for triplicate analyses were 0.7 ‰ for hydrogen and 0.09 ‰ for oxygen.

*2.6 Calculations and Statistics*

The hydrogen isotope ratios ($^2H/^1H$) of individual samples were normalized to the VSMOW scale and reported as $\delta^2H$ values, where $\delta^2H = (((^2H/^1H)_{sample}/(^2H/^1H)_{VSMOW})) - 1$, and is multiplied by 1000 to express in terms of ‰ (Coplen, 2011). The apparent $^2H/^1H$ fractionation factor between lipids and source water was calculated as $\alpha^2_{Lipid/Water} = (^2H/^1H)_{Lipid}/(^2H/^1H)_{Water}$. Because $\delta^2H_{water}$ values were consistent among batch cultures, we used the mean $\delta^2H$ value (-82.8 ± 0.7 ‰) to calculate $\alpha^2_{Lipid/Water}$ values from all cultures. Although $\alpha^2_{Lipid/Water}$ is the aggregate isotope effect of several biochemical steps and may differ due to kinetic isotope fractionation across a wide range of $\delta^2H_{water}$ values, it serves as a useful representation of apparent $^2H/^1H$ fractionation (Sessions and Hayes, 2005; Zhang et al.,

2014). The relative offset in $\delta^2H$ values among lipids was calculated as $\varepsilon^2_{\text{Lipid 1/Lipid 2}}$ (= $\alpha^2_{\text{Lipid 1/Lipid 2}} - 1$), and is multiplied by 1000 to express in terms of ‰.

Comparisons of $\delta^2H_{\text{lipid}}$, $\alpha^2_{\text{lipid-water}}$ values, and $\varepsilon^2_{\text{Lipid 1/ Lipid 2}}$ values among taxonomic groups were made with Brown-Forsythe and Welch one-way ANOVA tests, with posthoc Dunnett's T3 multiple comparisons test to assess pairwise comparisons among taxonomic groups. Ordinary least squares regression was used to compare $\alpha^2_{\text{lipid-water}}$ values and $\varepsilon^2_{\text{Lipid 1/ Lipid 2}}$ values from the ponds with chlorophyll *a* concentrations and the relative biovolumes of different algal taxonomic groups. All statistical analyses were performed in Prism (Version 9.5.1, GraphPad Software, LLC).

## 3. Results

### *3.1 Hydrogen isotope fractionation in algal cultures varies among compound classes and taxonomic groups*

The variability in $\delta^2H$ values for individual lipids among different cultures was large (> 200 ‰), even though $\delta^2H_{\text{water}}$ values were constant, indicating a wide range of species-specific $\alpha^2_{\text{Lipid/Water}}$ values (**Figure 1**). $\alpha^2_{\text{Lipid/Water}}$ values clustered by taxonomic class, with green algae having higher $\alpha^2_{\text{C16:0/Water}}$ values than any other group (**Figure 1a**). Green algae also tended to produce relatively $^2H$-enriched phytol, especially relative to phytol from cyanobacteria (**Figure 1b**). However, the difference in $\delta^2H_{\text{Phytol}}$ values between green algae and diatoms was less pronounced than the difference in their respective $\delta^2H_{\text{C16:0}}$ values, and dinoflagellates and cryptomonads had similar $\delta^2H_{\text{Phytol}}$ values to green algae (**Figure 1b**). In the case of sterols, those from diatoms were significantly enriched in $^2H$ relative to all three other groups of eukaryotic phytoplankton (**Figure 1c**), in marked contrast to the relatively low $\alpha^2_{\text{C16:0/Water}}$ and $\alpha^2_{\text{Phytol/Water}}$ values from diatoms.

Among algal taxonomic groups, there were also clear differences in the relative $^2H/^1H$ offset among biomarkers from different compound classes ($\varepsilon^2_{\text{Lipid 1/Lipid 2}}$ values) (**Figure 1**). Green algae and cyanobacteria tended to have relatively high $\varepsilon^2_{\text{C16:0/Phytol}}$ values compared to the remaining eukaryotic algal groups (**Figure 1d**). While the difference in mean $\varepsilon^2_{\text{C16:0/Phytol}}$ values among groups was large (> 100 ‰), it was not significant. Diatoms had the lowest $\varepsilon^2_{\text{C16:0/Sterols}}$ values of any group, while green algae tended to have the highest (although these were not significantly different from those of dinoflagellates) (**Figure 1e**). Diatoms had the highest $\varepsilon^2_{\text{Sterol/Phytol}}$ and dinoflagellates had the lowest, with intermediate values for green

algae and cryptomonads (**Figure 1f**). The overall magnitude of variability for $\varepsilon^2_{C16:0/Sterols}$ values among all eukaryotic taxa was roughly twice as large as that of $\varepsilon^2_{Sterol/Phytol}$ values.

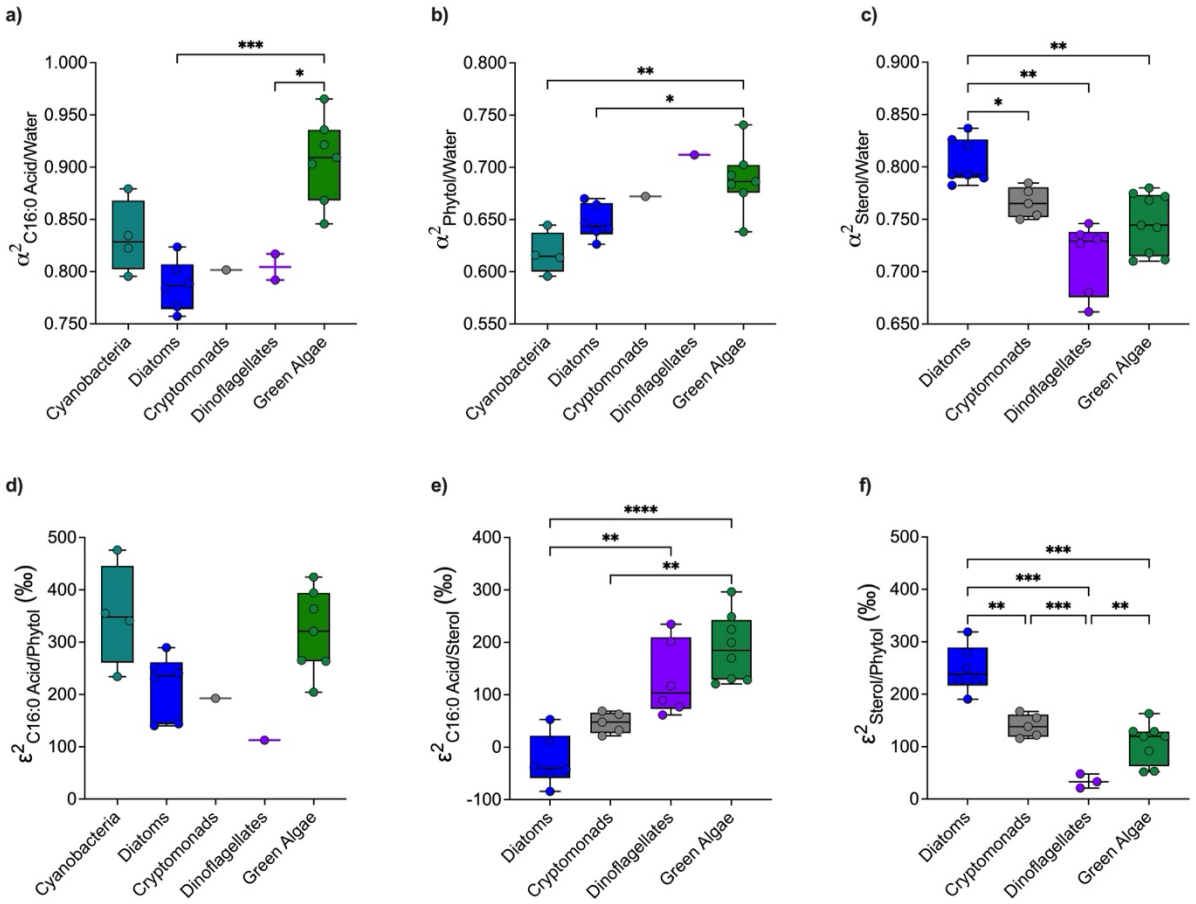


**Figure 1** Hydrogen isotope variability among lipids from algal batch cultures. Panels a, b, and c show $\alpha^2_{Lipid/Water}$ values for C16:0 fatty acid, phytol, and all measured sterols, respectively. The y-axes of panels a, b, and c are scaled to span a range of 0.250, but the absolute values differ among panels to accommodate different $\alpha^2_{lipid/water}$ values for each compound. Panels d, e, and f show relative $^2H/^1H$ offsets ($\varepsilon^2_{Lipid\ 1/Lipid\ 2}$ values) between C16:0 fatty acid and phytol, C16:0 fatty acid and sterol, and sterols and phytol, respectively. The y-axes of panels d, e, and f are scaled to span a range of 500 ‰, but the absolute values differ among panels to accommodate different $\varepsilon^2_{Lipid\ 1/Lipid\ 2}$ values for each compound. $*p < 0.05$; $**p < 0.01$; $***p < 0.001$; $****p < 0.0001$.

*3.2 Hydrogen isotope fractionation varied with nutrient additions to experimental ponds for some compounds*

Pond water isotopes became progressively enriched in $^2H$ and $^{18}O$ as the experiment progressed due to evaporation, but had minimal variation among ponds each week (**Table 1**). Overall, $\delta^2H_{Water}$ values from the final sampling week were within ~ 10 ‰ of those from the first sampling week. Despite this relatively small range of $\delta^2H_{Water}$ values, $\delta^2H_{Lipid}$ values for individual compounds spanned a much larger range, > 150 ‰ in the case of some fatty acids.

The magnitude of variability in $\alpha^2_{Lipid/Water}$ values was not consistent among compounds, even for those we were able to measure in almost all samples. For example, the standard deviation for $\alpha^2_{C16:0\ Acid/Water}$ values was 0.043 (n = 58), while $\alpha^2_{Phytol/Water}$ values had a standard deviation of 0.012 (n = 53).

**Table 1.** Mean water isotope values for pond water during each sampling week (n = 20 for each week). Uncertainty represents one standard deviation of all measurements.

| Date | $\delta^2$H (VSMOW, ‰) | $\delta^{18}$O (VSMOW, ‰) |
|---|---|---|
| 23.08.2016 | -37.4 ± 1.6 | -3.4 ± 0.3 |
| 13.09.2016 | -32.4 ± 0.9 | -2.2 ± 0.2 |
| 05.10.2016 | -29.9 ± 1.0 | -1.7 ± 0.2 |

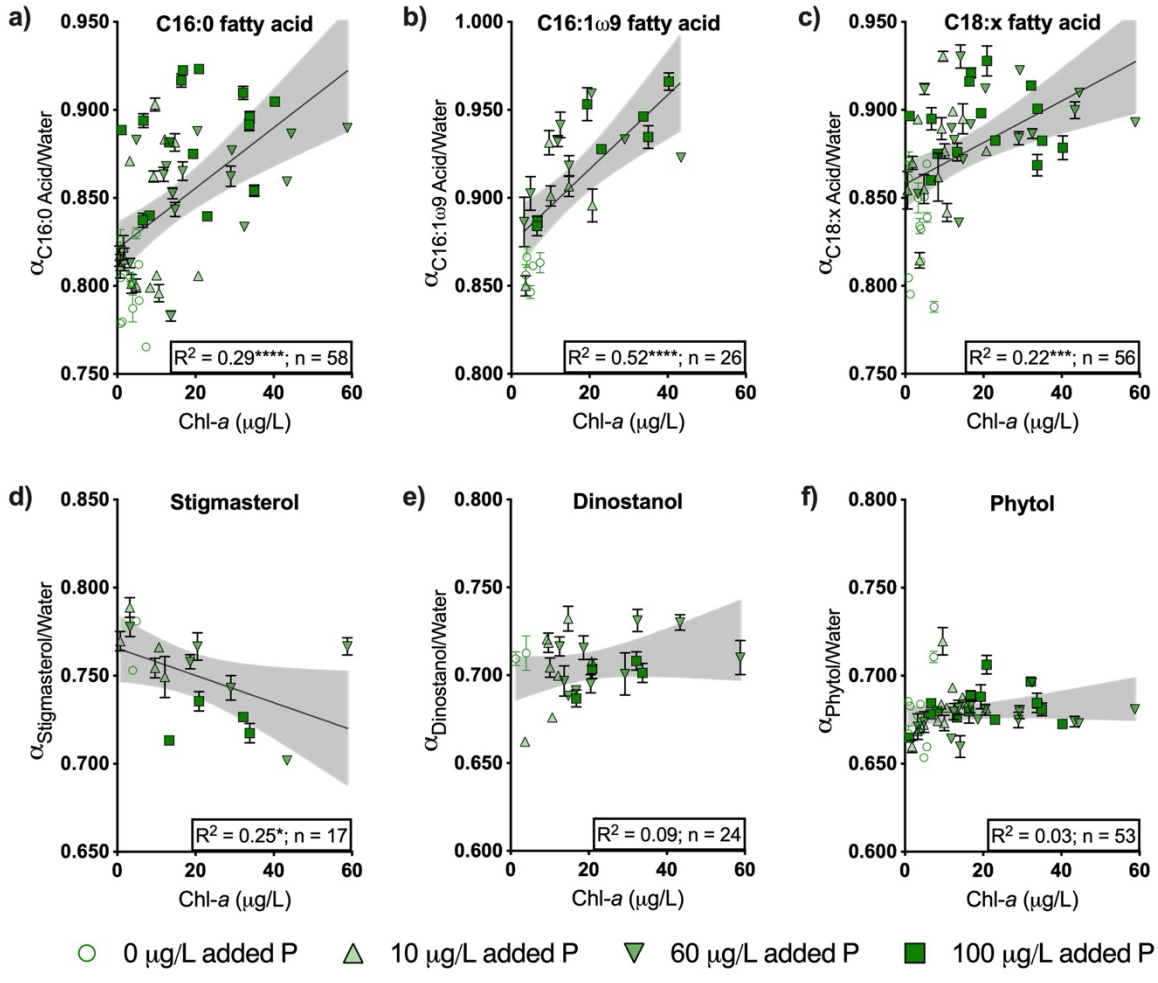


**Figure 2** Relationships between $\alpha^2_{Lipid/Water}$ values and chlorophyll *a* concentration in experimental ponds for selected compounds. Symbols represent total cumulative added P. Ponds that were designated oligotrophic controls (0 µg/L added P) are represented with open circles regardless of sampling week. For all other treatments, upward-facing triangles represent samples collected on August 23rd, downward-facing triangles represent samples

collected on September 13, and squares represent samples collected on October 5, 2016. Shading represents 95 % confidence intervals of linear regressions. Regression lines are shown for significant linear correlations. *$p < 0.05$; ***$p < 0.001$; ****$p < 0.0001$.

For several compounds, including more generic fatty acids such as $C_{16:0}$, $C_{16:1}$, and $C_{18:x}$, $\alpha^2_{Lipid/Water}$ values were positively correlated with overall algal productivity in the pond experiment, as indicated by chlorophyll *a* concentration (**Figure 2**). In contrast to these fatty acids, $\alpha^2_{Lipid/Water}$ values for stigmasterol, the sterol which we were able to measure $\delta^2H$ values from in the greatest number of ponds, were negatively correlated with algal productivity. For other compounds, including phytol and the dinoflagellate biomarker dinostanol, there was no correlation between $\alpha^2_{Lipid/Water}$ values and productivity indicators (**Figure 2**).

In the experimental ponds, nutrient loading and the presence and/or absence of keystone species not only caused overall algal productivity to vary, but also resulted in changes in the relative abundance of different algal taxa, as explored in more detail by Narwani et al. (2019). In many cases, $\varepsilon^2_{Lipid\ 1/Lipid\ 2}$ values varied with changes in algal community composition that were consistent with the results of the unialgal batch cultures. For example, in ponds where the algal biovolume was dominated by cyanobacteria and/or green algae, $\varepsilon^2_{C16:0/Phytol}$ values were higher than in ponds where these two taxa were less abundant (**Figure 3a**), consistent with the pattern identified in the batch cultures (Figure 1d). Likewise, $\varepsilon^2_{C16:0/Stigmasterol}$ values were positively correlated with the relative abundance of green algae (**Figure 3b**), again, consistent with the batch cultures (**Figure 1e**). There was a negative trend for $\varepsilon^2_{Stigmasterol/Phytol}$ values as the relative abundance of green algae increased, but this correlation was not significant (**Figure 3c**).

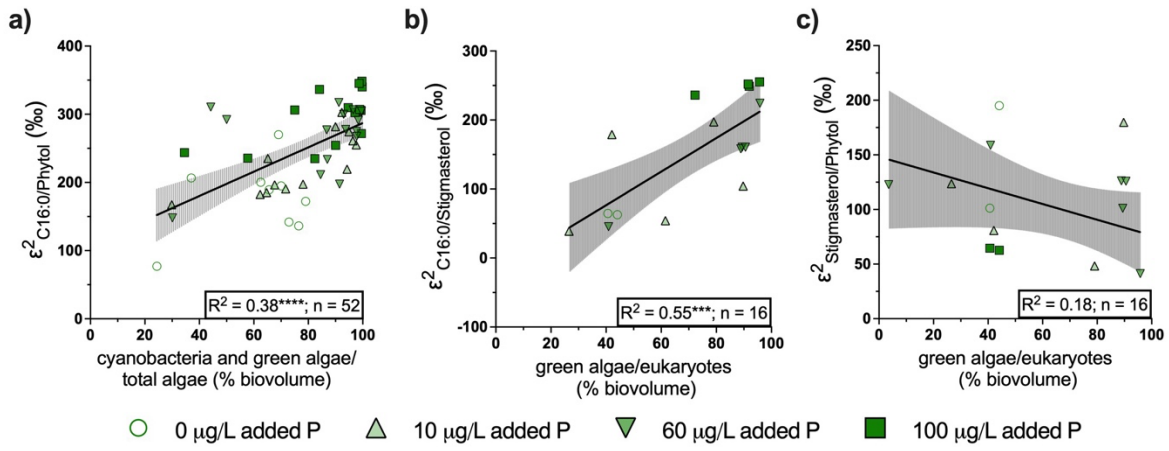


**Figure 3** Relationships between $\varepsilon^2_{Lipid\ 1/Lipid\ 2}$ values and changes in the relative abundance of algal groups for selected compound pairs. Panel a shows the relationship between $\varepsilon^2_{C16:0/Phytol}$

values and the relative abundance of cyanobacteria and green algae (as a percentage of the total algal biovolume). Panel b shows the relationship between $\varepsilon^2_{C16:0/Stigmasterol}$ values and the relative abundance of green algae (as a percentage of the total eukaryotic algal biovolume), panel c shows the equivalent relationship for $\varepsilon^2_{Stigmasterol/Phytol}$ values (note different scaling for y-axis in panel c). Cyanobacteria are excluded from the biovolume in panels b and c as they do not produce sterols. Symbols represent total cumulative added P. Ponds that were designated oligotrophic controls (0 μg/L added P) are represented with open circles regardless of sampling week. For all other treatments, upward-facing triangles represent samples collected on August 23rd, downward-facing triangles represent samples collected on September 13, and squares represent samples collected on October 5, 2016. Shading represents 95 % confidence intervals of linear regressions; regression lines are only shown for significant correlations. ***$p < 0.001$, ****$p < 0.0001$.

## 4. Discussion

We determined how hydrogen isotope fractionation between lipids and source water varied among algae in batch cultures of 20 species representing five taxonomic groups, and assessed how changes in algal community composition in experimental ponds related to changes in net hydrogen isotope fractionation for both ubiquitous and relatively source-specific lipids. Our results indicate that variability in biosynthetic hydrogen isotope fractionation is large compared to the natural variability of hydrogen isotopes in the global water cycle. They also suggest that there are systematic differences in biosynthetic hydrogen isotope fractionation among algal taxonomic groups that differ among lipid compound classes. In the following discussion, we explore potential biochemical mechanisms that may account for these patterns, demonstrate how the relative abundance of different algal species can affect the net hydrogen isotope signal recorded by ubiquitous algal lipids, and propose a conceptual framework for disentangling changes in algal community composition from changes in source water hydrogen isotopes in sedimentary records.

### *4.1 Sources of variability in hydrogen isotope fractionation factors among algal taxa*

Many of the differences in $\alpha^2_{Lipid/Water}$ values for phytol and sterols that we observed among algal taxonomic groups in batch cultures are consistent with existing knowledge about sources of variability in biosynthetic hydrogen isotope fractionation during the synthesis of isoprenoid lipids. Although the hydrogen in the lipids of photosynthesizing organisms is originally from the water in which they grew, various biochemical reactions result in $^2H/^1H$ fractionation and impact the overall $\delta^2H$ values of lipids (Sessions et al., 1999; Session and Hayes, 2005; Sachse et al., 2012). In particular, contributions from NADPH produced by different reactions have a large influence on lipid $\delta^2H$ values (X. Zhang et al., 2009; Cormier

et al., 2018; Wijker et al., 2019). NADPH produced in photosystem 1 in the chloroplast is depleted in $^2$H by several hundred ‰ relative to NAD(P)H formed during glycolysis or by the oxidative pentose phosphate cycle (Schmidt et al., 2003; X. Zhang et al. 2009; Cormier et al., 2018). As such, processes that impact the relative contributions of hydride from distinct NADPH sources represent one of the main mechanisms by which biosynthetic $\alpha^2_{Lipid/Water}$ values can vary on large scales (Sachs and Kakwa, 2015; Maloney et al., 2016; Cormier et al., 2018; Ladd et al., 2021b).

Previous observations of variability in $\alpha^2_{Lipid/Water}$ values for phytol and sterols have frequently been attributed to differences in the relative contributions from each of two biosynthetic pathways – the cytosolic mevalonic acid (MVA) pathway and the plastidic methylerythritol phosphate (MEP) pathway – that can produce isoprenoids (**Figure 4**) (Sessions et al., 1999; Sachse et al., 2012; Maloney et al., 2016; Sachs et al., 2016, 2017; Ladd et al., 2018, 2021b). Compounds produced by the MEP pathway, including phytol, tend to be depleted in $^2$H relative to compounds produced in the MVA pathway, most likely due to relatively more H from photosynthetic NADPH being incorporated into MEP derived isoprenoids (Sessions et al., 1999; Chikaraishi et al., 2004; Sessions, 2006; Zhou et al., 2011; Ladd et al., 2021b; Rhim et al., 2023). Although specific compounds tend to be produced by one pathway or the other (e.g., phytol by the MEP pathway and sterols by the MVA pathway), they contain common biosynthetic precursors that can be produced by both pathways, and that are likely exchanged across the plastid membrane (Hemerlin et al., 2012; Ladd et al., 2021b, 2023) (**Figure 4**). Most eukaryotic algae produce isoprenoids using both the MVA and the MEP pathway, but green algae are only capable of producing isoprenoids, including sterols, through the MEP pathway (Schwender et al., 1996; Disch et al., 1998; Lichtenthaler, 1999). As such, green algae would be expected to have lower $\alpha^2_{Sterol/Water}$ values than other eukaryotic algae. Consistent with this expectation, green algae in our culturing data set have lower $\alpha^2_{Sterol/Water}$ values than diatoms (**Figure 1c**).

Dinoflagellates in our cultures also had relatively low $\alpha^2_{Sterol/Water}$ values (**Figure 1c**), even though they have the genetic capability to produce sterols through the MVA pathway (Hemerlin et al., 2012). However, transcriptomic data indicate that many dinoflagellates rely exclusively on the MEP pathway for isoprenoid synthesis (Bentlage et al., 2016). Low $\alpha^2_{Sterol/Water}$ values for dinosterol and other sterols produced by dinoflagellates are consistent with a tendency for dinoflagellates to produce sterols via the MEP pathway, resulting in $\alpha^2_{Sterol/Water}$ values that are comparable to those from green algae, which are obliged to use the MEP pathway for sterol synthesis. The low $\alpha^2_{Sterol/Water}$ values observed in our dinoflagellate

cultures are consistent with values for the dinoflagellate biomarker dinostanol in the pond samples (**Figure 2**), as well as with those reported from environmental dinosterol (Nelson and Sachs, 2014; Schwab et al., 2015; Maloney et al., 2019), a sterol primarily produced by dinoflagellates (Volkman, 2003). For example, in surface sediments and suspended organic matter filtered from the water column of saline and hypersaline lakes, $\alpha^2_{Dinosterol/Water}$ values were consistently lower than $\alpha^2_{Brassicasterol/Water}$ values from the same samples (Nelson and Sachs, 2014). The freshwater end member value for $\alpha^2_{Dinosterol/Water}$ in this study was 0.688, which is within the range we observed for dinoflagellates in our cultures (**Figure 1c**) and similar to measurements of $\alpha^2_{Dinosterol/Water}$ from suspended organic matter in lakes in Cameroon (0.713 ± 0.011; Schwab et al., 2015). These low $\alpha^2_{Sterol/Water}$ values for sterols produced by dinoflagellates, along with expression of MEP genes but not MVA genes in several dinoflagellate taxa (Bentlage et al., 2016), provide additional support for the hypothesis that relative use of the MEP pathway for sterol precursors is a primary driver of variability in $\alpha^2_{Sterol/Water}$ values.

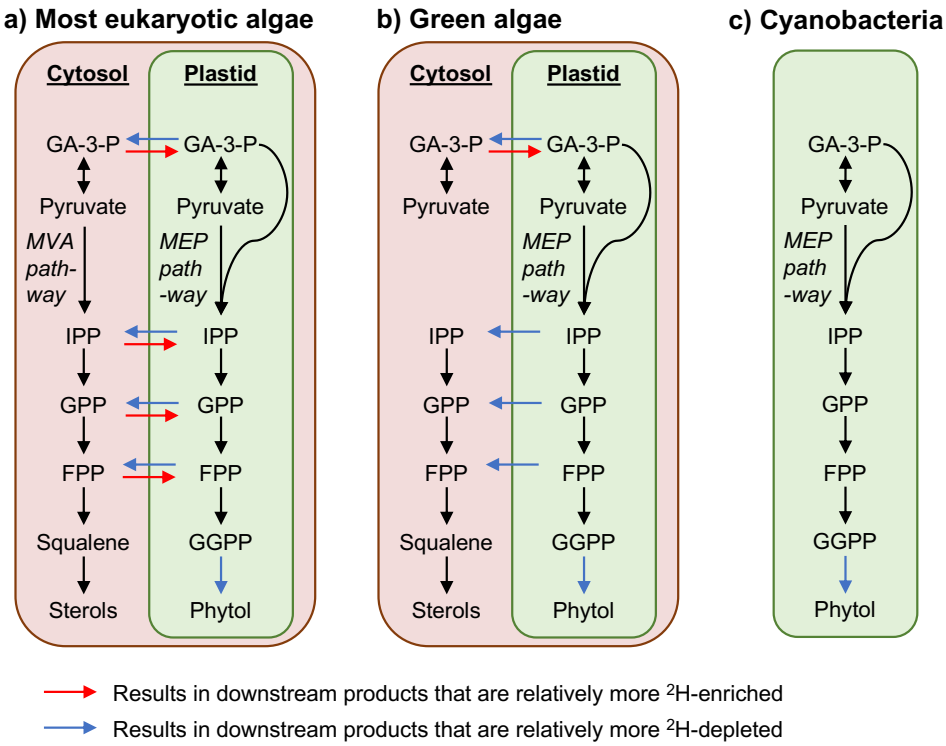


**Figure 4:** Schematic representation of biochemical steps that could result in $^2$H-enrichment or depletion for isoprenoid lipids in (a) eukaryotic microalgae other than green algae, (b) green algae, and (c) cyanobacteria. Several intermediate compounds are omitted for clarity. Abbreviations: FPP, farnesyl pyrophosphate; GA-3-P, glyceraldehyde 3-phosphate; GGPP, geranylgeranyl pyrophosphate; GPP, geranyl pyrophosphate; IPP isopentenyl pyrophosphate; MEP, methylerythritol phosphate; MVA, mevalonic acid.

In contrast to sterols, phytol is typically produced via the MEP pathway (Hemerlin et al., 2012) (**Figure 4**). Low $\alpha^2_{Phytol/Water}$ values, relative to those from sterols and other isoprenoids, are typically attributed to phytol's MEP source (Sessions et al., 1999; Sessions, 2006; Ladd et al., 2021b). Our algal cultures and experimental pond samples were also characterized by low $\alpha^2_{Phytol/Water}$ values (**Figure 1b, 2f**). Notably, $\alpha^2_{Phytol/Water}$ values were always lower than $\alpha^2_{Sterol/Water}$ values from the same sample, indicated by positive $\varepsilon^2_{Sterol/Phytol}$ values. This relationship is observed even for cultures of taxa that cannot (green algae) or apparently do not (dinoflagellates) produce sterols via the MVA pathway (**Figure 1f**). Therefore, low $\alpha^2_{Phytol/Water}$ values cannot be attributed solely to phytol's production in the MEP pathway. Additional $^2$H-depletion of phytol relative to MEP-derived sterols is likely caused by the addition of extremely $^2$H-depleted hydrogen during the hydrogenation of geranylgeranyl pyrophosphate (GGPP) to form phytol (Chikaraishi et al., 2009) (**Figure 4**). The only reported $\varepsilon^2_{GGPP/Phytol}$ values are from cucumber cotyledons, and have a value of 98 ‰ (Chikaraishi et al., 2009), comparable to $\varepsilon^2_{Sterol/Phytol}$ values of 89 ± 53 ‰ from cultured green algae and dinoflagellates, and to $\varepsilon^2_{Sterol/Phytol}$ values of ~85 ‰ from higher plants that produce sterols primarily with MEP-derived precursors (Ladd et al., 2021b). As such, differences between sterol and phytol $\delta^2$H values (as non-zero $\varepsilon^2_{Sterol/Phytol}$ values) from green algae and dinoflagellates are likely caused only by hydrogenation of GGPP to phytol, while the higher $\varepsilon^2_{Sterol/Phytol}$ values from cultured diatoms (221 ± 47 ‰) likely represent the combined H-isotope effects of GGPP hydrogenation and sterol synthesis via the MVA pathway (**Figure 4**).

Phytol $\delta^2$H values were lowest in cultured cyanobacteria (**Figure 1b**). Cyanobacteria only produce isoprenoids via the MEP pathway and lack the MVA pathway, therefore there is no possibility that cyanobacterial phytol is synthesized from MVA intermediates. In most eukaryotic algae, metabolic cross-talk of isoprenoid intermediates across the plastid membrane has the potential to contribute relatively $^2$H-enriched precursors to phytol synthesis, as a significant portion of phytol in higher plants can be from MVA-derived precursors (Opitz et al., 2014), and the same is likely true for phytol in eukaryotic algae that maintain both pathways. However, crosstalk between the MEP and MVA pathways cannot explain why green algae also produce phytol that is enriched in $^2$H relative to phytol from cyanobacteria, since these eukaryotes also lack the MVA pathway. Another possible mechanism by which $^2$H-enriched cytosolic precursors could be incorporated into phytol in

eukaryotes is via transport of glyceraldehyde 3-phospate (GA-3-P) into the plastid, where it could substitute for relatively $^{2}$H-depleted GA-3-P produced from the Calvin Cycle (**Figure 4**) (Ladd et al., 2021b). Incorporation of cytosolic GA-3-P into plastidic isoprenoids could explain $^{2}$H-enrichment of phytol from all eukaryotes relative to phytol from cyanobacteria, and thus seems like the more plausible explanation to account for this difference.

It is less apparent why fatty acid $\delta^{2}$H values would be higher in green algae than in other taxa (**Figure 1a**). Differences in the metabolism of green algae relative to diatoms and other eukaryotes, including the nature of their plastid membranes (Archibald, 2015; Zulu et al., 2018) and NADPH transfer between chloroplasts and mitochondria (Bailleul et al., 2015) could potentially shift the relative sources of carbohydrate precursors and/or NADPH used in fatty acid synthesis, thereby affecting overall $\alpha^{2}_{\text{Fatty Acid/Water}}$ values. From our present data, we are only able to observe that this $^{2}$H-enrichment of green algal fatty acids seems to be robust, with consistent $\alpha^{2}_{\text{Fatty Acid/Water}}$ values for green algal cultures and for ponds that became dominated by green algae. Future experimental work should investigate the mechanistic causes of relatively $^{2}$H-enriched fatty acids in green algae, relative to other taxa. Ideally, these follow-up experiments will incorporate complementary metabolomic and transcriptomic analyses, which could also be used to test the hypotheses we have presented for variable $\alpha^{2}_{\text{Lipid/Water}}$ values during isoprenoid synthesis by different taxonomic groups.

### *4.2 Changes in algal community composition can lead to large changes in net $^{2}H/^{1}H$ fractionation for common algal lipids*

Similar to our measurements from algal batch cultures and experimental ponds, field studies of hydrogen isotope fractionation associated with common lipids in Swiss lakes have reported a wide range in $\alpha^{2}_{\text{C16:0/Water}}$ values, with an overall smaller range and lower values for $\alpha^{2}_{\text{Phytol/Water}}$ values (Ladd et al., 2017; Ladd et al., 2018). For example, in a time series of algal biomass collected from Greifensee, $\alpha^{2}_{\text{C16:0/Water}}$ values ranged from 0.743 to 0.891, while $\alpha^{2}_{\text{Phytol/Water}}$ values ranged from 0.617 to 0.668 (Ladd et al., 2017). The design of these field studies left it uncertain whether this variability in $\alpha^{2}_{\text{Lipid/Water}}$ values was due to variability within taxa as environmental variables such as temperature or nutrient availability changed, or if it was due to changes in community composition. Our new batch culture data demonstrates that the range in fractionation factors due to species composition alone is enough to account for natural variability in $\alpha^{2}_{\text{Lipid/Water}}$ values, and the taxonomic variability is an order of magnitude larger than within-species variability driven by environmental

variables such as salinity, temperature, light levels, and nutrient availability (e.g., Schouten et al., 2006; Zhang and Sachs, 2007; Sachs and Kawka, 2015; van der Meer et al., 2015; Maloney et al., 2016).

The experimental pond results demonstrate how compositional variability of algal communities can lead to large shifts in $\alpha^2_{\text{Fatty Acid/Water}}$ values. Due to nutrient additions and interactions with keystone species, the algal community composition among the different ponds diverged, with green algae and cyanobacteria becoming much more dominant in some ponds than others (Narwani et al., 2019). Both of these taxa have higher $\alpha^2_{\text{Fatty Acid/Water}}$ values than other cultured algae (**Figure 1a**), and it would thus be expected that $\alpha^2_{\text{Fatty Acid/Water}}$ values increase in ponds where they dominate, as we observed in the ponds, albeit with some scatter (**Figure 2a-c**).

The expected signal for changes in $\alpha^2_{\text{Phytol/Water}}$ values is more complicated, since green algae had higher values than diatoms, while cyanobacteria had a non-significant tendency towards lower values than diatoms (**Figure 1b**). The smaller range and minimal trend in $\alpha^2_{\text{Phytol/Water}}$ values in the ponds is thus also consistent with the culturing results (**Figure 2f**). In the case of stanols and sterols, $\alpha^2_{\text{Lipid/Water}}$ values for dinostanol, which is not produced by green algae nor cyanobacteria, were insensitive to changing community composition (**Figure 2e**), while those for stigmasterol, which is produced by cryptomonads, dinoflagellates, and green algae (Volkman, 2003; Taipale et al., 2016; Peltomaa et al., 2023), decreased in the more productive ponds (**Figure 2d**), consistent with the relatively low $\alpha^2_{\text{Sterol/Water}}$ values from green algae in culture (**Figure 1c**).

Changes in algal community composition seem more likely to explain the observed changes in $\alpha^2_{\text{Lipid/Water}}$ values in the ponds than other potential explanations. Higher nutrient concentrations are unlikely to explain higher $\alpha^2_{\text{Fatty/Water}}$ values, since higher growth rates and/or higher nutrient concentrations typically result in lower or constant $\alpha^2_{\text{Lipid/Water}}$ values in cultured algae (Schouten et al., 2006; Z. Zhang et al., 2009; Sachs and Kawka, 2015; Wolhowe et al., 2015). Second, although many common fatty acids, including C16:0, are also produced by heterotrophic microbes and zooplankton, changes in relative contributions from heterotrophs would be expected to produce a decrease in $\alpha^2_{\text{Lipid/Water}}$ values for fatty acids in ponds with greater algal productivity. Fatty acids synthesized through heterotrophic metabolisms typically have higher $\alpha^2_{\text{Fatty Acid/Water}}$ values than those synthesized from photosynthetic products (X. Zhang et al., 2009; Osburn et al., 2011; Heinzelmann et al., 2015; Cormier et al., 2018). Algal blooms are therefore expected to result in lower $\alpha^2_{\text{Fatty Acid/Water}}$ values, as a higher percentage of the fatty acids will be derived from photoautotrophs

(Heinzelmann et al., 2016). Decreases in $\alpha^2_{\text{Fatty Acid/Water}}$ values during periods of increased chlorophyll concentrations have in fact been observed in time series of suspended particles from the water column in the North Sea (Heinzelmann et al., 2016) and in lakes from central Switzerland (Ladd et al., 2017), opposite to the trend observed in the ponds with the largest algal blooms.

Mixotrophy can also affect $\alpha^2_{\text{Fatty Acid/Water}}$ values (Cormier et al., 2022). Since mixotrophy becomes a more dominant strategy under low nutrient conditions (Stoecker et al., 2017; Wentzky et al., 2020), it should result in higher $\alpha^2_{\text{Fatty acid/Water}}$ values in less productive ponds, the opposite of the observed trend (**Figure 2**). Additionally, the maximum effect of mixotrophy within a single species across extreme conditions (green algae grown in the dark on glucose compared to green algae grown in the light without glucose in the medium) is only a ~ 0.040 change in $\alpha^2_{\text{Fatty Acid/Water}}$ values (Cormier et al. 2022), considerably smaller than the ~ 0.120 variability in $\alpha^2_{\text{Fatty Acid/Water}}$ values among ponds (**Figure 2**). As such, mixotrophy, heterotrophy, and changes in growth rate within individual taxa are all unlikely to explain the large variability $\alpha^2_{\text{Fatty Acid/Water}}$ values that occurred in our pond experiment.

### *4.3 Interpreting $\delta^2H$ values of multiple lipid biomarkers in sediments*

Lipid $\delta^2H$ values may be much more sensitive to taxonomic compositional changes in the algal community than to changes in water $\delta^2H$ values, especially for compounds with a diverse range of producers. As such, there is potential to develop $\delta^2H$ values of lipids as paleoecological indicators, which would be particularly useful for constraining the past abundance of taxonomic groups that are underrepresented in traditional microscopic techniques, including most green algae, and would be complementary to pigment analyses, where interpretation is challenging due to variability in the degradation rates among pigments produced by different taxa. In practice, the use of lipid $\delta^2H$ values as ecological indicators will be most useful when comparing changes in the relative $^2H$-offsets among different compounds (that is, $\varepsilon^2_{\text{Lipid 1/Lipid 2}}$ values), as these are insensitive to changes in water $\delta^2H$ values, which will have a secondary impact on the $\delta^2H$ values of individual compounds.

In the pond experiment, we observed that $\varepsilon^2_{\text{Lipid 1/Lipid 2}}$ values for different lipid pairs often changed in the way we would have predicted based on the culturing results. In particular, $\varepsilon^2_{\text{C16/Phytol}}$ values increased in the ponds where a greater percentage of the algal biovolume was from green algae and cyanobacteria (**Figure 3a**). In ponds where all or almost all of the algal biovolume was from green algae and cyanobacteria, $\varepsilon^2_{\text{C16/Phytol}}$ values were

~300 ‰, similar to the $\varepsilon^2_{C16/Phytol}$ values from these two taxonomic groups in cultures (**Figure 1d**). These two compounds are produced by virtually all algae, and thus may be most appropriate for capturing changes in the relative contributions from different taxonomic groups. Likewise, in the context of considering $\varepsilon^2_{Sterol/Phytol}$ and $\varepsilon^2_{C16/Sterol}$ values as ecological indicators, it is more useful to make calculations with a sterol that is produced by diverse algae, rather than a relatively source specific organism. Among the compounds we were able to analyze from the ponds, stigmasterol is a relatively common sterol produced by some cryptomonads, diatoms, dinoflagellates, and green algae (Volkman, 2003; Taipale et al., 2016; Peltomaa et al., 2023). Based on the culturing data, $\varepsilon^2_{C16/Stigmasterol}$ values should increase as green algal biovolume increases, exactly as observed in the ponds (**Figure 3b**). At the same time, this shift should produce lower $\varepsilon^2_{Stigmasterol/Phytol}$ values, which we observed as a non-significant trend in the ponds (**Figure 3c**).

Ecological effects on lipid $\delta^2H$ values have the potential to be much larger than typical changes in precipitation isotopes, which at mid-latitudes vary by ~50 ‰ across large climate reorganizations such as glacial-interglacial transitions (Tierney et al., 2020). Despite the potential ecological complications, in many circumstances it is still possible to infer changes in past water $\delta^2H$ values from sedimentary $\delta^2H$ values. In general, the more source-specific a lipid biomarker is, the more likely changes in its hydrogen isotope composition are to reflect changes in source water hydrogen isotopes, rather than changes in ecology. For example, dinosterol $\delta^2H$ values are positively correlated with lake water and precipitation $\delta^2H$ values in freshwater lakes on Pacific islands, while $C_{16:0}$ acid $\delta^2H$ values from the same sediments are not (Maloney et al., 2019; Ladd et al., 2021a). The highest confidence that sedimentary $\delta^2H$ signals are driven primarily by changes in precipitation $\delta^2H$ values can be achieved by measuring $\delta^2H$ values of two lipids and calculating their $\varepsilon^2_{Lipid\ 1/Lipid\ 2}$ values (**Figure 5**). If the $\varepsilon^2_{Lipid\ 1/Lipid\ 2}$ values are relatively stable, it is strongly suggestive that changes in the individual lipid $\delta^2H$ values are primarily driven by source water $\delta^2H$ values. This is true for two relatively source specific lipids, two generic lipids from different biosynthetic pathways, or a combination of the two. On the other hand, fluctuating $\varepsilon^2_{Lipid\ 1/Lipid\ 2}$ values between two lipids are indicative of change in the relative contributions from different source organisms, which can either be used simply to identify non-hydrologic components of sediment record, or to reconstruct algal community dynamics provided adequate background on the ecological setting. Overall, measuring lipid $\delta^2H$ values from a wide range of compounds within a single

sediment sample, and calculating $^{2}H$-offsets among them, offers an opportunity to reconstruct changes in hydroclimate and aquatic ecology over time.

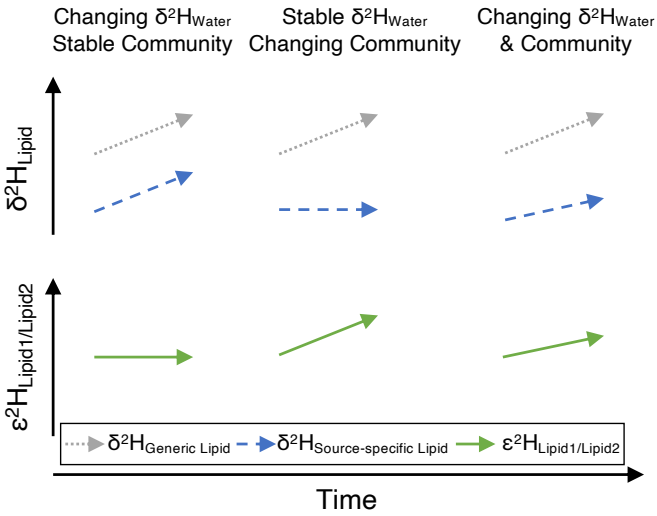


**Figure 5** Schematic representation of how $\delta^{2}H_{Lipid}$ values and $\varepsilon^{2}_{Lipid\ 1/Lipid\ 2}$ values may change over time in response to changes in $\delta^{2}H_{Water}$ values and algal community composition. Positive trends in arrows are generally representative of change, and in real sediments could be negative, non-linear, or influenced by low-amplitude stochastic variability.

## 5. Conclusions

Hydrogen isotope fractionation during lipid synthesis varies among algal species, but these differences have not previously been systematically explored as a (paleo)ecological indicator. Here, we cultured 20 species of phytoplankton, representing cyanobacteria, diatoms, green algae, dinoflagellates, and cryptomonads, and measured the $\delta^{2}H$ values of their fatty acids, sterols, and phytol. We observed that $\delta^{2}H_{Lipid}$ values differed among taxonomic groups, and that the relative abundance of $^{2}H$ in lipids of different compound classes also displays distinct patterns among taxonomic groups. For example, diatoms produced relatively $^{2}H$-depleted fatty acids and relatively $^{2}H$-enriched sterols, with green algae displaying the opposite pattern. As such, the relative $^{2}H$-offsets between different lipids, expressed as $\varepsilon^{2}_{Lipid\ 1/Lipid\ 2}$ values, is highly sensitive to taxonomic source, and can be developed as a proxy of community composition that is independent to changes in source water $\delta^{2}H$ values. We subsequentially demonstrated how $\varepsilon^{2}_{Lipid\ 1/Lipid\ 2}$ values change with community composition through an ecosystem manipulation in 20 experimental ponds. These results can be applied to interpret sedimentary variability in $\delta^{2}H_{Lipid}$ values of co-occurring compounds. In sediment records, changes in $\delta^{2}H_{Lipid}$ values of highly source-specific lipids,

or synchronized changes in $\delta^2H_{Lipid}$ values of lipids of different compounds with diverse biological sources, can be interpreted as changes in $\delta^2H_{Water}$ values. Changes in the $\varepsilon^2_{Lipid\ 1/Lipid\ 2}$ values of common lipids with broad taxonomic sources, on the other hand, can be used to identify past changes in algal community composition.

**Acknowledgements**

This research was funded by a US National Science Foundation postdoctoral fellowship to SNL (EAR-1452254), a Swiss National Science Foundation Eccellenza fellowship to SNL (PCEFP2_194211), and Eawag internal funds to AN, BM, and CJS. Hannele Penson assisted with sampling from experimental ponds. Serge Robert and Anton Hertler assisted with laboratory analyses of lipid samples. Daniel Montluçon measured water isotopes.

**Appendix A. Supplementary Material**

A list of cultured algal species and their taxonomic classification (**Table S1**) is included at the end of this manuscript.

**Author contributions**

Conceptualization: SNL, DBN, BM, CJS; Data curation: SNL, DBN, AN; Formal analysis: SNL, DBN, AK; Funding acquisition: SNL, BM, AN, CJS; Investigation: SNL, DBN, SD, RL; Project coordination: SNL, BM, AN; Resources: AN, ND, CJS; Supervision: ND, CJS; Visualization: SNL; Writing – original draft: SNL; Writing – review and editing: All

**Data availability**

All lipid and water $\delta^2H$ values generated as part of this study are available through the Dryad Digital Repository (https://doi.org/10.5061/dryad.nvx0k6f0v). Additional data from the pond experiment, including algal cell counts, biovolume, and water chemistry, is available through the Dryad Digital Repository (https://doi.org/10.5061/dryad.qv9s4mw99).

**References**

Archibald, J.M., 2015. Genomic perspectives on the birth and spread of plastids. Proc. Natl. Acad. Sci. U. S. A. 112, 10147-10153.

Bailleul, B., Berne, N., Murik, O., Petroutsos, D., Prihoda, J., Tanaka, A., Villanova, V., Bligny, R., Flori, S., Falconet, D., Krieger-Liszkay, A., Santabarbara, S., Rappaport, F., Joliot, P., Tirichine, L., Falkowski, P.G., Cardol, P., Bowler, C., Finazzi, G., 2015. Energetic coupling between plastids and mitochondria drives $CO_2$ assimilation in diatoms. Nature 524, 366–369.

Bauersachs, T., Talbot, H.M., Sidgwick, F., Sivonen, K., Schwark, L., 2017. Lipid biomarker signatures as tracers for harmful cyanobacterial blooms in the Baltic Sea. PLoS ONE 12, e0186360.

Bentlage, B., Rogers, T.S., Bachvaroff, T.R., Delwiche, C.F., 2016. Complex ancestries of isoprenoid synthesis in dinoflagellates. J. Eukaryotic Microbiol. 63, 123–137.

686 Bianchi, T.S., Rolff, C., Widbom, B., Elmgren, R., 2002. Phytoplankton pigments in Baltic
687 Sea seston and sediments: seasonal variability, fluxes, and transformations. Estuarine,
688 Coastal Shelf Sci. 55, 369–383.
689 Boere, A.C., Rijpstra, W.I.C., de Lange, G.J., Sinninghe Damsté, J.S., Coolen, M.J.L., 2011.
690 Preservation potential of ancient plankton DNA in Pleistocene marine sediments.
691 Geobiology 9, 377–393.
692 Casteñada, I.S., Schouten, S., 2011. A review of molecular organic proxies for examining
693 modern and ancient lacustrine environments. Quat. Sci. Rev. 30, 2851–2891.
694 Chikaraishi, Y., Naraoka, H., Poulson, S.R., 2004. Hydrogen and carbon isotopic
695 fractionations of lipid biosynthesis among terrestrial (C3, C4 and CAM) and aquatic
696 plants. Phytochemistry 65, 1369–1381.
697 Chikaraishi, Y., Tanaka, R., Tanaka, A., Ohkouchi, N., 2009. Fractionation of hydrogen
698 isotopes during phytol biosynthesis. Org. Geochem. 40, 569–573.
699 Coplen, T.B., 2011. Guidelines and recommended terms for expression of stable-isotope-ratio
700 and gas-ratio measurement results. Rapid Commun. Mass Spectrom. 25, 2538–2560.
701 Cormier, M.-A., Werner, R.A., Sauer, P.E., Grocke, D.R., Leuenberger, M.C., Wieloch, T.,
702 Schleucher, J., Kahmen, A., 2018. $^{2}$H-fractionations during the biosynthesis of
703 carbohydrates and lipids imprint a metabolic signal on the $\delta^{2}$H values of plant organic
704 compounds. New Phytol. 218, 479–491.
705 Cormier, M.-A., Berard, J.-B., Bougaran, G., Tureman, C.N., Mayer, D.J., Lampitt, R.S.,
706 Kruger, N.J., Flynn, K.J., Rickaby, R.E.M., 2022. Deuterium in marine organic
707 biomarkers: toward a new tool for quantifying aquatic mixotrophy. New Phytol. 234,
708 776–782.
709 Diaz, R.J., Rosenberg, R., 2008. Spreading dead zones and consequences for marine
710 ecosystems. Science 321, 926–929.
711 Disch, A., Schwender, J., Müller, C., Lichtenthaler, H.K., Rohmer, M., 1998. Distribution of
712 the mevalonate and glyceraldehyde phosphate/pyruvate pathways for isoprenoid
713 biosynthesis in unicellular algae and the cyanobacterium *Synechocystis* PCC 6714.
714 Biochem. J. 333, 381–388.
715 Dixit, A.S., Dixit, S.S., Smol, J.P., 1992. Algal microfossils provide high temporal resolution
716 of environmental trends. Water, Air, Soil Pollut. 62, 75–87.
717 Gosling, W.D., Sear, D.A., Hassall, J.D., Langdon, P.G., Bönnen, M.N.T., Driessen, T.D.,
718 van Kemenade, Z.R., Noort, K., Leng, M.J., Croudace, I.W., Bourne, A.J.,
719 McMichael, C.N.H., 2020. Human occupation and ecosystem change on Upolu
720 (Samoa) during the Holocene. J. Biogeogr. 47, 600–614.
721 Guillard, R.R.L., Lorenzen, C.J., 1972. Yellow-green algae with chlorophyllide c. J. Phycol. 8,
722 10–14.
723 Haas, M., Baumann, F., Castella, D., Haghipour, N., Reusch, A., Strasser, M., Eglington, T.I.,
724 Dubois, N., 2019. Roman-driven cultural eutrophication of Lake Murten, Switzerland.
725 Earth Planet. Sci. Lett. 505, 110–117.
726 Heinzelmann S.M., Villanueva L., Sinke-Schoen D., Sinninghe Damsté J.S., Schouten S.,
727 van der Meer M.T.J., 2015. Impact of metabolism and growth phase on the hydrogen
728 isotopic composition of microbial fatty acids. Front. Microbiol. 6, 408.
729 Heinzelmann S.M., Bale N.J., Villanueva L., Sinke-Schoen D., Philippart C.J.M., Sinninghe
730 Damsté J.S., Smede J., Schouten S. van der Meer M.T.J., 2016. Seasonal changes in
731 the D/H ratio of fatty acids of pelagic microorganisms in the coastal North Sea.
732 Biogeosciences 13, 5527–5539.

Hemmerlin A., Harwood J.L., Bach, T.J., 2012. A raison d'être for two distinct pathwys in the early steps of plant isoprenoid biosynthesis? Prog. Lipid Res. 51, 95–148.

Hixon, S.M., Arts, M.T., 2016. Climate warming is predicted to reduce omega-3, long-chain, polyunsaturated fatty acid production in phytoplankton. Global Change Biol. 22, 2744–2755.

Huang Y., Shuman B., Wang Y., Webb III T., 2004. Hydrogen isotope ratios of individual lipids in lake sediments as novel tracers of climatic and environmental change: a surface sediment test. J. Paleolimnol. 31, 363–375.

Huisman, J., Codd, G.A., Paerl, H.W., Ibelings, B.W., Verspagen, J.M.H., Visser, P.M., 2018. Cyanobacterial blooms. Nat. Rev. Microbiol. 16, 471–483.

Kirkpatrick, J.B., Walsh, E.A., D'Hondt, S., 2016. "Fossil DNA persistence and decay in marine sediment over hundred-thousand-year to million-year time scales. Geology 44, 615–618.

Krentscher, C., Dubois, N., Camperio, G., Prebble, M., Ladd S.N., 2019. Palmitone as a potential species-specific biomarker for the crop plant taro (*Colocasia esculenta* Schott) on remote Pacific islands. Org. Geochem. 132, 1–10.

Ladd, S.N., Dubois, N., and Schubert, C.J., 2017. Interplay of community dynamics, temperature, and productivity on the hydrogen isotope signatures of lipid biomarkers. Biogeosciences 14, 3979–3994.

Ladd, S.N., Nelson, D.B., Schubert, C.J., Dubois, N., 2018. Lipid compound classes display diverging hydrogen isotope responses in lakes along a nutrient gradient. Geochim. Cosmochim. Acta 237, 103–119.

Ladd, S.N., Maloney, A.E., Nelson, D.B., Prebble, M., Camperio, G., Sear, D.A., Hassall, J., Langdon, P.G., Sachs, J.P., Dubois, N., 2021. Leaf wax hydrogen isotopes as a hydroclimate proxy in the tropical Pacific. J. Geophys. Res.: Biogeosci. 126, e2020JG005891.

Ladd, S.N., Nelson, D.B., Bamberger, I., Daber, L.E., Kreuzwieser, J., Kahmen, A., Werner, C., 2021b. Metabolic exchange between pathways for isoprenoid synthesis and implications for biosynthetic hydrogen isotope fractionation. New Phytol. 231, 1708–1719

Ladd, S.N., Daber, L.E., Bamberger, I., Kübert, A., Kreuzwieser, J., Purser, G., Ingrisch, J., Deleeuw, J., van Haren, J., Meredith, L.K., Werner, C., 2023. Leaf-level metabolic changes in response to drought affect daytime $CO_2$ emission and isoprenoid synthesis pathways. Tree Physiol. 43, 1917–1932.

Leavitt, P.R., Findlay, D.L., 1994. Comparison of fossil pigments with 20 years of phytoplankton data from eutrophic Lake 227, Experimental Lakes Area, Ontario. Can. J. Fish. Aquat. Sci. 51, 2286–2299.

Leavitt P.R., Hodgson D.A., 2002. Sedimentary pigments, in: Smol J.P., Birks H.J.B., Last W.M., Bradley R.S., Alverson K. (Eds.) Tracking Environmental Change Using Lake Sediments. Developments in Paleoenvironmental Research, vol 3. Springer, Dordrecht, Netherlands, pp. 295–325.

Lichtenthaler, H.K., 1999. The 1-Deoxy-D-Xylulose-5-Phosphate pathway of isoprenoid biosynthesis in plants. Ann. Rev. Plant Phys. 50, 47–65.

Livingstone, D., Jaworski, G.H.M., 1980. The viability of akinetes of blue-green algae recovered from the sediments of rostherne mere. Br. Phycol. J. 15, 357–364.

Lotter, A.F., 1998. The recent eutrophication of Baldeggersee (Switzerland) as assessed by fossil diatom assemblages. The Holocene 8, 395–405.

Lürig, M.D., Narwani, A., Penson, H., Wehrli, B., Spaak, P., Matthews, B., 2021. Non-additive effects of foundation species determine the response of aquatic ecosystems to nutrient perturbation. Ecology 102, e03371.

Maloney, A.E., Shinneman, A.L., Hemeon, K., Sachs, J.P., 2016. Exploring lipid 2 H/1 H fractionation mechanisms in response to salinity with continuous cultures of the diatom *Thalassiosira pseudonana*. Org. Geochem. 101, 154–165.

Maloney, A.E., Nelson, D.B., Richey, J.N., Prebble, M., Sear, D.A., Hassell, J.D., Langdon, P.G., Croudace, I.W., Zawadzki, A., Sachs, J.P., 2019. Reconstructing precipitation in the tropical South Pacific from dinosterol $^{2}H/^{1}H$ ratios in lake sediment. Geochim. Cosmochim. Acta 245, 190–206.

Markelov I., Couture, R.-M., Fischer, R., Haande, S., Van Cappellen, P., 2019. Coupling water column and sediment biogeochemical dynamics: modeling internal Phosphorus lading, climate change responses, and mitigation measures in Lake Vansjo, Norway. J. Geophys. Res.: Biogeosci. 124, 3847–3866.

McGowan, S., Barker, P., Haworth, E.Y., Leavitt, P.R., Maberly, S.C., Pates, J., 2012. Humans and climate as drivers of algal community change in Windermere since 1850. Freshwater Biol. 57, 260–277.

Meyers, P.A., 1997. Organic geochemical proxies of paleoceanographic, paleolimnologic, and paleoclimatic processes. Org. Geochem. 27, 213–250.

Monchamp, M., Spaak, P., Domaizon, I., Dubois, N., Bouffard, D., Pomati, F., 2018. Homogenization of lake cyanobacterial communities over a century of climate change and eutrophication. Nat. Ecol. Evol. 2, 317–324.

Naeher, S., Smittenberg, R.H., Gilli, A., Kirilova, E.P., Lotter, A., Schubert, C.J., 2012. Impact of recent lake eutrophication on microbial community change as revealed by high resolution lipid biomarkers in Rotsee (Switzerland). Org. Geochem. 49, 86–95.

Narwani, A., Reyes, M., Pereira, A.L., Penson, H., Dennis, S.R., Derrer, S., Spaak, P., Matthews, B., 2019. Interactive effects of foundation species on ecosystem functioning and stability in response to disturbance. Proc. R. Soc. B 286, 20191857.

Nelson D.B., Sachs J.P., 2014. The influence of salinity on D/H fractionation in dinosterol and brassicasterol from globally distributed saline and hypersaline lakes. Geochim. Cosmochim. Acta 133, 325–339.

Nwosi, E.C., Brauer, A., Monchamp, M.-E., Pinkerneil, S., Bartholomäus, A., Theuerkauf, M., Schmidt, J.-P., Stoof-Leichsenring, K.R., Wietelmann, T., Kaiser, J., Wagner, D., Liebner, S., 2023. Early human impact on lake cyanobacteria revealed by a Holocene record of sedimentary ancient DNA. Commun. Biol. 6, 72.

Opitz, S., Nes, W.D., Gershenzon, J., 2014. Both methylerythritol phosphate and mevalonate pathways contribute to biosynthesis of each of the major isoprenoid classes in young cotton seedlings. Phytochemistry 98, 110–119.

Osburn M.R., Sessions A.L., Pepe-Ranney C., Spear J.R., 2011. Hydrogen-isotopic variability in fatty acids from Yellowstone National Park hot spring microbial communities. Geochim. Cosmochim. Acta 75, 4830–4845.

Pawlowski, J., Kelly-Quinn, M., Altermatt, F., Apothéloz-Perret-Gentil, L., Beja, P., Boggero, A., Borja, A., Bouchez, A., Cordier, T., Domaizon, I., Feio, M.J., Filipe, A.F., Fornaroli, R., Graf, W., Herder, J., van der Hoorn, B., Jones, J.I., Sagova-Mareckova, M., Moritz, C., Barquín, J., Piggott, J.J., Pinna, M., Rimet, F., Rinkevich, B., Sousa-Santos, C., Specchia, V., Trobajo, R., Vasselon, V., Vitecek, S., Zimmermann, J. Weigand, A., Leese, F., Kahlert, M.. 2018. The future of biotic indices in the ecogenomic era: Integrating (e)DNA metabarcoding in biological assessment of aquatic ecosystems. Sci. Total Environ. 637-638, 1295–1310.

Peltomaa, E., Asikainen, H., Blomster, J., Pakkanen, H., Rigaud, C., Salmi, P., Taipale, S., 2023. Phytoplankton group identification with chemotaxonomic biomarkers: In combination they do better. Phytochemistry 209, 113624.

Rabalais, N.N., Diaz, R.J., Levin, L.A., Turner, R.E., Gilbert, D., Zhang, J., 2010. Dynamics and distribution of natural and human-caused hypoxia. Biogeosciences 7, 585–619.

Reuss, N., Conley, D.J., Bianchi, T.S., 2005. Preservation conditions and the use of sedimentary pigments as a tool for recent ecological reconstruction in four Northern European estuaries. Mar. Chem. 95, 283–302.

Rhim, J.H., Kopf, S., McFarlin, J., Batther, H., Harris, C.M., Zhou, A., Feng, X., Weber, Y., Hoeft-McCann, S., Pearson, A., Leavitt, W.D., 2023. The hydrogen isotope signatures of autotrophy versus heterotrophy recorded in archeal tetraether lipids. bioRxiv, doi: 10.1101/2023.11.29.569324

Sachs, J.P., Kawka, O.E., 2015. The influence of growth rate on 2 H/1 H fractionation in continuous cultures of the coccolithophorid *Emiliania huxleyi* and the diatom *Thalassiosira pseudonana*. PloS ONE 10, e0141643.

Sachs, J.P., Maloney, A.E., Gregersen, J., Paschall, C., 2016. Effect of salinity on $^{2}H/^{1}H$ fractionation in lipids from continuous cultures of the coccolithophorid *Emiliania huxleyi*. Geochim. Cosmochim. Acta 189, 96–109.

Sachs, J.P., Maloney, A.E., Gregersen, J., 2017. Effect of light on 2H/1H fractionation in lipids from continuous cultures of the diatom *Thalassiosira pseudonana*. Geochim. Cosmochim. Acta 209, 204–215.

Sachse, D., Radke, J., Gleixner, G., 2004. Hydrogen isotope ratios of recent lacustrine sedimentary *n*-alkanes record modern climate variability. Geochim. Cosmochim. Acta 68, 4877–4889.

Sachse, D., Sachs, J., 2008. Inverse relationship between D/H fractionation in cyanobacterial lipids and salinity in Christmas Island saline ponds. Geochim. Cosmochim. Acta 72, 793–806.

Sachse, D., Billault, I., Bowen, G.J., Chikaraishi, Y., Dawson, T.E., Feakins, S.J., Freeman, K.H., Magill, C.R., McInerney, F.A., Van der Meer, M.T.J., Polissar, P., Robins, R.J., Sachs, J.P., Schmidt, H., Sessions, A.L., White, J.W.C., West, J.B., Kahmen, A., 2012. Molecular paleohydrology: interpreting the hydrogen-isotope composition of lipid biomarkers from photosynthesizing organisms. Annu. Rev. Earth Planet. Sci. 40, 221–249.

Schimmelmann, A., Sessions, A.L., Mastalerz, M., 2006. Hydrogen isotopic (D/H) composition of organic matter during diagenesis and thermal maturation. Annu. Rev. Earth Planet. Sci. 34, 501–533.

Schmidt, H.L., Werner, R., Eisenreich, W., 2003. Systematics of $^{2}H$ patterns in natural compounds and its importance for the elucidation on biosynthetic pathways. Phytochem. Rev. 2, 61–85.

Schouten, S., Ossebaar, J., Schreiber, K., Kienhuis, M.V.M., Langer, G., Benthien, A., Bijma, J., 2006. The effect of temperature, salinity and growth rate on the stable hydrogen isotopic composition of long chain alkenones produced by *Emiliania huxleyi* and *Gephyrocapsa oceanica*. Biogeosciences 3, 113–119.

Schubert, C.J., Villanueva, J., Calvert, S.E., Cowie, G.L., von Rad, U., Schulz, H., Berner, U., Erlenkeuser, H., 1998. Stable phytoplankton community structure in the Arabian Sea over the past 200,000 years. Nature 394, 563-566.

Schwab, V.F., Garcin, Y., Sachse, D., Todou, G., Séné, O., Onana, J., Achoundong, G., Gleixner, G., 2015. Dinosterol δD values in stratified tropical lakes (Cameroon) are affected by eutrophication. Org. Geochem. 88, 35–49.

Schwender, J., Seemann, M., Lichtenthaler, H.K., Rohmer, M., 1996. Biosynthesis of isoprenoids (carotenoids, sterols, prenyl side–chains of chlorophylls and plastoquinone) via a novel pyruvate/glyceraldehyde 3–phosphate non–mevalonate pathway in the green alga *Scenedesmus obliquus*. Biochem. J. 316, 73–80.

Sessions, A.L., Burgoyne, T.W., Schimmelmann, A., Hayes, J.M., 1999. Fractionation of hydrogen isotopes in lipid biosynthesis. Org. Geochem. 30, 1193–1200.

Sessions, A.L., Hayes, J.M., 2005. Calculation of hydrogen isotopic fractionations in biogeochemical systems. Geochim. Cosmochim. Acta 69, 593–597.

Sessions, A.L., 2006. Seasonal changes in D/H fractionation accompanying lipid biosynthesis in *Spartina alterniflora*. Geochim. Cosmochim. Acta 70, 2153–2162.

Stoecker, D.K., Hansen, P.J., Caron, D.A., Mitra, A., 2017. Mixotrophy in the marine plankton. Annu. Rev. Mar. Sci. 9, 311–335.

Stoermer, E.F., Wolin, J.A., Schelske, C.L., Conley, D.J., 1985. An assessment of ecological changes during the recent history of Lake Ontario based on siliceous algal microfossils preserved in sediments. J. Phycol. 21, 257–276.

Stoof-Leichsenring, K.R., Herzschuh, U., Pestryakova, L.A., Klemm, J., Epp, L.S., Tiedemann, R., 2015. Genetic data from algae sedimentary DNA reflect the influence of environment over geography. Sci. Rep. 5, 12924.

Strivins, N., Soininen, J., Tonno, I., Freiberg, R., Veski, S., Kisand, V., 2018. Towards understanding the abundance of non-pollen palynomorphs: a comparison of fossil algae, algal pigments and sedaDNA from temperate northern lake sediments. Rev. Palaeobot. Palynol. 249, 9–15.

Taipale, S.J., Hiltunen, M., Vuorio, K., Peltomaa, E., 2016. Suitability of phytosterols alongside fatty acids as chemotaxonomic biomarkers for phytoplankton. Front. Plant Sci. 7, 212.

Thorpe, A.C., Mackay, E.B., Goodall, T., Bendle, J.A., Thackeray, S.J., Maberly, S.C., Read, D.S., 2024. Evaluating the use of lake sedimentary DNA in palaeolimnology: A comparison with long-term microscopy-based monitoring of the phytoplankton community. Mol. Ecol. Resour. 24, e13903.

Tierney, J.E., Zhu, J., King, J., Malevich, S.B., Hakim, G.J., Poulsen, C.J., 2020. Glacial cooling and climate sensitivity revisited. Nature 584, 569–573.

van der Meer M.T.J., Benthien A., French K.L., Epping E., Zondervan I., Reichart G.J., Bijma J., Sinninghe Damsté J.S., Schouten,S. 2015. Large effect of irradiance on hydrogen isotope fractionation of alkenones in *Emiliania huxleyi*. Geochim. Cosmochim. Acta 160, 16–24.

Vasselon, V., Bouchez, A., Rimet, F., Jacquet, S., Trobajo, R., Corniquel, K., Domaizon, I., 2018. Avoiding quantification bias in metabarcoding: Application of a cell biovolume correction factor in diatom molecular biomonitoring. Methods Ecol. Evol. 9, 1060–1069.

Volkman J.K., 2003. Sterols in microorganisms. Appl. Microbiol. Biotechnol. 60, 495–506.

Weiss, G.M., Schouten, S., Sinninghe Damsté, J.S., van der Meer, M.T.J., 2019. Constraining the application of hydrogen isotopic composition of alkenones as a salinity proxy using marine surface sediments. Geochim. Cosmochim. Acta 250, 34–48.

Wentzky, V.C., Tittel, J., Jäger, C.G., Bruggeman, J., Rinke, K., 2020. Seasonal succession of functional traits in phytoplankton communities and their interaction with trophic state. J. Ecol. 108, 1649–1663.

Wijker, R.S., Sessions, A.L., Fuhrer, T., Phan, M., 2019. 2H/1H variation in microbial lipids is controlled by NADPH metabolism. Proc. Natl. Acad. Sci. U. S. A. 116, 12173–12182.

Witkowski, C.R., Weijers, J.W.H., Blais, B., Schouten, S., Sinninghe Damsté, J.S., 2018. Molecular fossils from phytoplankton reveal secular $P_{CO2}$ trend over the Phanerozoic. Sci. Adv. 4, eaat4556.

Wolhowe, M.D., Prahl, F.G., Langer, G., Oviedo, A.M., Ziveri, P. 2015. Alkenone δD as an ecological indicator: A culture and field study of physiologically-controlled chemical and hydrogen-isotopic variation in $C_{37}$ alkenones. Geochim. Cosmochim. Acta 162, 166–182.

Zhang, Z., Sachs, J.P., 2007. Hydrogen isotope fractionation in freshwater algae: 1. Variations among lipids and species. Org. Geochem. 38, 582–608.

Zhang, X., Gillespie, A., Sessions, A.L., 2009. Large D/H variations in bacterial lipids reflect central metabolic pathways. Proc. Natl. Acad. Sci. U. S. A. 106, 12580–12586.

Zhang, Z., Sachs, J.P., Marchetti, A., 2009. Hydrogen isotope fractionation in freshwater and marine algae: II. Temperature and nitrogen limited growth rate effects. Org. Geochem. 40, 428–439.

Zhang, Z., Nelson, D.B., Sachs, J.P., 2014. Hydrogen isotope fractionation in algae: III. Theoretical interpretations. Org. Geochem. 75, 1–7.

Zhou, Y., Grice, K., Chikaraishi, Y., Stuart-Williams, H., Farquhar, G.D., Ohkouchi, N., 2011. Temperature effect on leaf water deuterium enrichment and isotopic fractionation during leaf lipid biosynthesis: Results from controlled growth of $C_3$ and $C_4$ land plants. Phytochemistry 72, 207–213.

Zulu, N.N., Zienkiewicz, K., Vollheyde, K., Feussner, I., 2018. Current trends to comprehend lipid metabolism in diatoms. Prog. Lipid Res. 70, 1–16.

**Table S1**: Cultured algal species and taxonomic classifications

| Species | Group | Class | Number of replicate cultures |
|---|---|---|---|
| *Achnanthes sp.* | diatoms | Bacillariophyceae | 3 |
| *Aphanizomenon flos-aquae* | cyanobacteria | Cyanophyceae | 3 |
| *Aphanothece clathrata* | cyanobacteria | Cyanophyceae | 3 |
| *Asterionella formosa* | diatoms | Bacillariophyceae | 2 |
| *Botryococcus braunii-1* | green algae | Trebouxiophyceae | 3 |
| *Botryococcus braunii-2* | green algae | Trebouxiophyceae | 3 |
| *Chlamydomonas reinhardtii* | green algae | Chlorophyceae | 3 |
| *Cosmarium botrytis* | green algae | Conjugatophyceae | 3 |
| *Cryptomonas ovata* | Cryptomonads | Cryptophyceae | 2 |
| *Cyclotella meneghiniana* | diatoms | Mediophyceae | 2 |
| *Cystodinium spec.* | dinoflagellates | Dinophyta | 2 |
| *Eudorina unicocca* | green algae | Chlorophyceae | 3 |
| *Microcystis aeruginosa* | cyanobacteria | Cyanophyceae | 2 |
| *Peridinium spec.* | dinoflagellates | Dinophyta | 2 |
| *Scenedesmus acuminatus* | green algae | Chlorophyceae | 3 |
| *Stephanodiscus minutulus* | diatoms | Bacillariophyceae | 3 |
| *Synechococcus* | cyanobacteria | Cyanophyceae | 5 |
| *Synedra rumpens var. familiaris* | diatoms | Bacillariophyceae | 2 |
| *Tabellaria sp.* | diatoms | Bacillariophyceae | 3 |
| *Volvox aureus* | green algae | Chlorophyceae | 3 |